Available online at www.sciencedirect.com
ScienceDirect
Geochimica et Cosmochimica Acta 71 (2007) 5605–5619
Geochimica et Cosmochimica Acta
www.elsevier.com/locate/gca

Reconciling kinetic and equilibrium observations of iron(III) solubility in aqueous solutions with a polymer-based model

Andrew L. Rose *, T. David Waite

Centre for Water and Waste Technology, School of Civil and Environmental Engineering, The University of New South Wales, Sydney, NSW 2052, Australia

Received 2 November 2006; accepted in revised form 26 February 2007; available online 4 September 2007

Abstract

Due to hydrolysis reactions, iron(III) forms oxyhydroxide precipitates in natural waters that minimise its availability to living organisms. Thermodynamic studies have established equilibrium concentrations of dissolved iron at various pH values, however these studies offer no insight into the kinetics of iron(III) polymerisation and subsequent precipitation. In recent work, the kinetics of iron(III) precipitation and dissolution of the precipitate have been investigated, but there are apparent discrepancies between the equilibrium solubility of iron(III) calculated from the kinetic parameters and its solubility measured by separation of the solid and dissolved phases at equilibrium. In this work, we reconcile kinetic and thermodynamic measurements using a polymer-based mechanistic model of the processes responsible for iron(III) precipitation in aqueous solutions based on a variety of previously published experimental data. This model is used to explain the existence of a solubility limit, including the effect of precipitate ageing on its solubility. We suggest that the model provides a unified approach for examining aqueous systems containing dissolved, solid-phase and surface species.

1. INTRODUCTION

Iron is rather interesting amongst the transition metal elements in that its thermodynamically stable Fe(III) state undergoes hydrolysis (i.e. deprotonation of water molecules coordinated in the inner sphere) in aqueous solutions in response to changing pH, leading to precipitation into a range of different solid forms even when it is present in relatively low concentrations. This property makes iron of interest to a wide range of scientists and engineers. For biogeochemists, the issue of how microorganisms obtain iron in the environment is a major question, given that it is needed by almost every living organism (Crichton, 2001) and yet is extremely insoluble near neutral pH. Geologists and geomicrobiologists are interested in what solid forms of iron are produced under different environmental conditions, and the mechanisms by which this occurs. Agricultural and environmental scientists are interested in the surface properties of iron precipitates and minerals, given their capacity to adsorb nutrients such as phosphate and contaminants such as arsenic. For engineers, Fe(III) precipitation is used as a means of coagulating colloidal particles and scavenging suspended and dissolved contaminants in water and wastewater treatment processes.

As a result of such widespread interest, a massive amount of work has been undertaken over the past half century and more investigating the phenomenon of Fe(III) precipitation in aqueous solution. This work has employed a range of experimental methods, each usually consistent with the aspect of Fe(III) precipitation that is of concern in a particular area of research. In spite of this, a great deal remains unknown about iron hydrolysis and precipitation, as reflected by continuing research in the fields mentioned above.

In the area of biogeochemistry, work has focussed largely on the solubility of Fe(III) in natural waters as a

* Corresponding author. Fax: +61 2 9313 8624.
E-mail address: andrew.rose@unsw.edu.au (A.L. Rose).

0016-7037/$ - see front matter © 2007 Elsevier Ltd. All rights reserved.
doi:10.1016/j.gca.2007.02.024

Glossary of symbols and abbreviations

Fe_i	Fe species (monomeric or polymeric) consisting of i Fe atoms in an unspecified arrangement
Fe'	sum of inorganic monomeric Fe species (equivalent to Fe_1)
FOP	sum of oligomeric and polymeric Fe species
n	number of Fe atoms in the largest polymer that can form, i.e. the total number of Fe atoms in the system
$[Fe]_T$	total concentration of Fe atoms in the system
$[Fe(x,y)_i]$	concentration of Fe atoms coordinated by x hydroxy-bridges and y oxy-bridges in a species with i Fe atoms in total
$[Fe(x,y)]_T$	total concentration of atoms coordinated by x hydroxy-bridges and y oxy-bridges in the system
$[Fe_{\leqslant p}]_T$	total concentration of Fe atoms in the form of either Fe′ or polymers containing at most p atoms
$[Fe']_0$	Fe′ concentration at pseudo-equilibrium immediately after polymerisation occurs in an initially homogeneous solution of Fe′
$\alpha_{Fe(OH)_3^0}$	proportion of Fe′ that is $Fe(OH)^0_{3(aq)}$ at a particular pH
$\alpha_{Fe(x,y)_i}$	proportion of atoms in a polymer Fe_i coordinated by x hydroxy-bridges and y oxy-bridges
$\alpha_{FOP\infty}$	limiting value for the proportion of Fe atoms available for reaction when bonded so as to minimise the number of available coordination sites
k_{fij}	second-order rate constant for the polymerisation reaction between two arbitrary species Fe_i and Fe_j ($M^{-1}\,s^{-1}$)
k_{fi}	second-order rate constant for the polymerisation reaction between Fe′ and an arbitrary species Fe_i ($M^{-1}\,s^{-1}$)
k_f	second-order rate constant for the polymerisation reaction between $Fe(OH)^0_{3(aq)}$ and Fe atoms in either Fe′ or a polymer ($M^{-1}\,s^{-1}$)
k^*_{f1}	conditional second-order rate constant for the homogeneous polymerisation reaction between two molecules of Fe′ at a particular pH ($M^{-1}\,s^{-1}$)
k^*_{fi}	conditional second-order rate constant for the heterogeneous polymerisation reaction between Fe′ and Fe atoms in a polymer Fe_i ($i > 1$) at a particular pH and for a particular distribution of Fe bonding arrangements in the polymer ($M^{-1}\,s^{-1}$)
$k^*_{f2\rightarrow n}$	conditional second-order rate constant for the heterogeneous polymerisation reaction between Fe′ and Fe atoms in all polymers at a particular pH and for a particular average distribution of Fe bonding over all polymers ($M^{-1}\,s^{-1}$)
k^*_f	conditional second-order rate constant for the polymerisation reaction between Fe′ and Fe atoms in either Fe′ or a polymer at a particular pH and for a particular average distribution of Fe bonding arrangements over all Fe species ($M^{-1}\,s^{-1}$)
k^*_{f0}	initial value of k^*_f as a function of time, corresponding to the greatest number of free coordination sites ($M^{-1}\,s^{-1}$)
$k^*_{f\infty}$	limiting (final) value of k^*_f as a function of time, corresponding to the least number of free coordination sites ($M^{-1}\,s^{-1}$)
k_{di}	first-order rate constant for detachment (dissolution or depolymerisation) of a Fe atom from an arbitrary polymer Fe_i (s^{-1})
$k_{dx,y}$	first-order rate constant for detachment of a Fe atom coordinated by x hydroxy-bridges and y oxy-bridges (s^{-1})
k^*_{di}	conditional first-order rate constant for detachment of a Fe atom from a polymer Fe_i at a particular pH and for a particular distribution of Fe bonding arrangements in the polymer (s^{-1})
k^*_d	conditional first-order rate constant for detachment of a Fe atom from a polymer at a particular pH and for a particular average distribution of Fe bonding arrangements over all Fe polymers (s^{-1})
k^*_{d0}	initial value of k^*_d as a function of time, corresponding to the greatest number of free coordination sites (s^{-1})
$k^*_{d\infty}$	limiting (final) value of k^*_d as a function of time, corresponding to the least number of free coordination sites (s^{-1})
K^*	pseudo-equilibrium (constant) value of the ratio k^*_{fi}/k^*_{di} (M^{-1})
k_1	first-order decay constant for the decrease in k^*_f and k^*_d due to a decrease in free coordination sites for Fe over time (s^{-1})
k_2	first-order decay constant for the decrease in k^*_d due to condensation of hydroxy-bridges to oxy-bridges over time (s^{-1})

function of commonly occurring environmental variables such as pH, ionic strength and temperature. A principal concern has been determining the solubility of iron(III) in natural waters as a function of pH by measuring the concentration of dissolved iron in equilibrium with the solid phase (Byrne and Kester, 1976; Kuma et al., 1992, 1993, 1996, 1998; Millero et al., 1995; Millero, 1998; Liu and Millero, 1999, 2002; Byrne et al., 2000; Sunda and Huntsman, 2003), mostly by separation of the phases using membranes. As techniques have been refined (for example due to the availability of membranes with smaller pore sizes), values for iron solubility have become more constrained. Sunda and Huntsman (2003) recently confirmed the accuracy of size-based solubility measurements using an approach based on adsorption of ^{59}Fe-labelled Fe(III) in equilibrium with EDTA complexes on to C_{18}–silica columns. Thus the solubility of iron in natural waters in the absence of organic ligands is now reasonably well known.

However, there remain several critical unresolved issues. Although there exist empirical equations to accurately describe Fe(III) solubility in seawater as a function of temperature, ionic strength and pH (Liu and Millero, 2002), there is ongoing debate about the interpretation of such data in terms of individual iron hydrolysis reactions. These data are usually modelled with four sequential deprotonation reactions of water molecules coordinated in the inner sphere of the Fe(III) atom:

$$[Fe^{III}(OH_2)_6]^{3+} \rightleftharpoons [Fe^{III}(OH_2)_5(OH)]^{2+} + H^+ \quad (1)$$

$$[Fe^{III}(OH_2)_5(OH)]^{2+} \rightleftharpoons [Fe^{III}(OH_2)_4(OH)_2]^{+} + H^+ \quad (2)$$

$$[Fe^{III}(OH_2)_4(OH)_2]^{+} \rightleftharpoons [Fe^{III}(OH_2)_3(OH)_3] + H^+ \quad (3)$$

$$[Fe^{III}(OH_2)_3(OH)_3]^{0} \rightleftharpoons [Fe^{III}(OH_2)_2(OH)_4]^{-} + H^+ \quad (4)$$

Perera and Hefter (2003) have also determined stability constants for the higher order hydrolysis reactions:

$$[Fe^{III}(OH_2)_2(OH)_4]^{-} \rightleftharpoons [Fe^{III}(OH_2)(OH)_5]^{2-} + H^+ \quad (5)$$

$$[Fe^{III}(OH_2)(OH)_5]^{2-} \rightleftharpoons [Fe^{III}(OH)_6]^{3-} + H^+ \quad (6)$$

They note that these reactions have typically been neglected in Fe(III) solubility studies, primarily because their existence was not well established, and that this may be at least partly responsible for the sub-optimal fit of equilibrium solubility models to data (Perera and Hefter, 2003). For example, the iron solubility versus pH relationship established by Liu and Millero (1999) in NaCl solution exhibits a slope that is greater than one above pH 9.5, suggesting the possible involvement of a di- or tri-anionic complex hydrolysis species. It has also been established that the presence of natural organic ligands at nanomolar concentrations can increase Fe(III) solubility (Kuma et al., 1996; Liu and Millero, 1999) (particularly around pH 8 where Fe(III) solubility is at its lowest), which can further confound data interpretation. Even when this is accounted for, effects of other common constituents of natural waters are usually not. For example, chloride, nitrate, sulphate, silicate and phosphate anions can participate in the Fe(III) precipitation process (Dousma et al., 1978, 1979; Rose et al., 1996, 1997a; Schwertmann et al., 1999; Doelsch et al., 2003), a fact that may also contribute to the sub-optimal fit of solubility models to data.

An additional factor that affects Fe(III) solubility is the "ageing" phenomenon, in which Fe(III) solubility decreases with time (Kuma et al., 1992, 1993; Liu and Millero, 1999, 2002). This indicates that systems in which Fe(III) solubility have been measured are not truly at equilibrium, and that a kinetic treatment is required to fully describe Fe(III) precipitation behaviour. Knowledge of precipitation and dissolution kinetics is also important because it is increasingly apparent that iron bioavailability is governed in many cases by kinetic factors, such as the competition for iron between organic ligands, membrane-associated ligands (proteins) in organisms and hydrolysis reactions (Sunda and Huntsman, 1998).

Kinetic studies of the reactions associated with iron precipitation have mostly examined dissolution (Kuma et al., 1992, 1993), and precipitation at low pH where such reactions occur relatively slowly (Grundl and Delwiche, 1993). We have examined Fe(III) precipitation kinetics around neutral pH (Rose and Waite, 2003; Pham et al., 2006), and determined rate constants for the loss of dissolved Fe(III) from solution that are consistent with an Eigen–Wilkins mechanism in which water loss from dissolved Fe(III) is the rate-limiting step in Fe(III) polymerisation and subsequent precipitation. However, rate constants obtained in this way lead to predictions of iron solubility around neutral pH that appear inconsistent (superficially, at least) with those obtained from equilibrium measurements (Rose and Waite, 2003).

In this work, we review the mechanism for Fe(III) hydrolysis and precipitation, and the reverse process of dissolution. We then synthesise this information into a polymer-based model, and use it to provide mechanistically consistent explanations for apparently disparate kinetic and equilibrium observations of Fe(III) solubility behaviour.

2. CONCEPTUAL FRAMEWORK

2.1. Definitions

Before attempting to conceptualise the processes of Fe(III) precipitation and dissolution, it is necessary to define exactly what is meant by solid precipitation and dissolution. *Precipitation* is the transformation of an element from the dissolved phase (in this case, the aqueous dissolved phase) to the solid phase. *Dissolution* is the reverse transformation of an element from the solid phase to the dissolved phase. It follows that we further need to define exactly what constitutes a transition from the solid phase to the dissolved phase. An *aqueous solution* is a mixture of water (the dominant component) and one or more other chemical components that are distributed throughout the mixture in a uniform manner. By uniform, we mean that there is an equal probability of any particular sample of the solution containing exactly the same components in the same proportion as any other sample of the solution, provided that the sample volume is physically large enough to contain at least one of each component of the solution. From the perspective of an aquatic chemist, the nature of the non-solution phase is not critical (it does not even need to be a solid); our major interest is when a particular species can no longer be considered to be dissolved.

We will consider that a substance is no longer dissolved when it is not uniformly distributed in solution, in the sense described above. In this work we will use the terms *dissolved* and *non-dissolved* strictly in accordance with this definition. As we will be making extensive use of concepts involved with polymer chemistry, we will also define associated terminology for clarity. In the context of aqueous iron chemistry, a *monomer* is a species containing one Fe atom, an *oligomer* is a species containing a small number of Fe atoms, and a *polymer* is a species containing a large number of Fe atoms. In terms of our definition of iron solubility, we consider monomers and oligomers to be dissolved, whereas polymers may either be dissolved or non-dissolved. For conciseness, we will use the term ferric oxyhydroxide polymer (FOP) to collectively refer to oligomeric and polymeric species of iron, while the abbreviation Fe′ will be used

conventionally to denote the sum of inorganic monomeric species. The exact composition of Fe′ varies depending on pH and the presence of various inorganic ions in the solution, but is assumed to reach equilibrium rapidly on the timescale of the other processes considered here, such that Fe′ always represents the equilibrium state of monomeric iron(III) under prevailing conditions.

Finally, as we intend to relate the polymer-based framework to existing observations of iron solubility, we must consider that iron solubility has traditionally been defined in terms of size (although this has typically been described as an "operational" rather than conceptual definition). On the basis of size, researchers have typically distinguished between *particulate* (>10 μm), *colloidal* (between 1 nm and 10 μm) and *truly dissolved* iron (<1 nm) (Stumm, 1992). It has widely been recognised that size-based determination of iron solubility suffers from some disadvantages, in particular that it is not possible to know what fraction of iron passing through a small pore-size filter can be considered dissolved from a chemical perspective (Kuma et al., 1998). We will not make any further attempt to distinguish dissolved and non-dissolved substances on the basis of size in this work, but note that a size-based distinction correlates only approximately with the concept that we have elucidated here. The relationship between a size-based definition of solubility and our definition based on the requirement for a uniform mixture is shown alongside the terminology associated with a polymer-based approach in Fig. 1.

2.2. Existing models for precipitation and dissolution

The majority of work on iron(III) precipitation and dissolution has focussed on the thermodynamics of iron(III) solubility. The traditional thermodynamic framework is based on the equilibrium reaction:

$$Fe(OH)_{3(s)} \rightleftharpoons Fe^{3+} + 3OH^- \quad (7)$$

The equilibrium constant is given as the product of the activities of the reaction products, divided by the product of the activities of the reactants. This equilibrium constant (the solubility product) does not involve the concentration of the solid, as the solid activity is deemed to be one (as is the activity of water), giving:

$$K_S = \{Fe^{3+}\}\{OH^-\}^3 \quad (8)$$

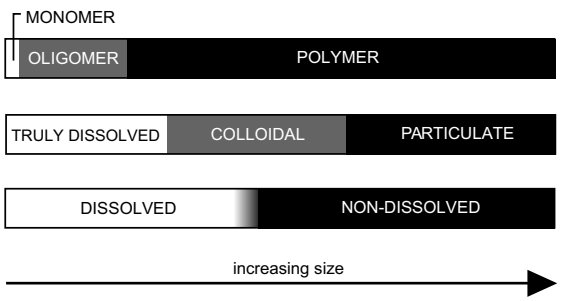

Fig. 1. Relationship between a size-based definition of solubility, a definition based on the requirement for a uniform mixture, and the polymer-based approach to solubility.

While this seems rather elementary, it hinges upon the definition of the activity of a solid as one. The implication of this definition is that a solid is completely separate from the solution and consequently behaves independently of reactions in solution, except for the equal exchange of iron between the solution and solid phases, due to the dynamic nature of equilibrium. If the right-hand side of Eq. (8) does not equal the left-hand side, then the solid is not in equilibrium with the solution; thus, if we know (or assume) the system to be at equilibrium, it follows that the solid cannot be present in this case. This leads to the concept of a solubility limit, in which at a particular pH (and hence a particular hydroxide activity), when $\{Fe^{3+}\} < K_S\{OH^-\}^{-3}$, all iron is dissolved and, conversely, when $\{Fe^{3+}\} = K_S\{OH^-\}^{-3}$ the activity of dissolved iron is constant, regardless of the total amount of iron in the system, due to the existence of the solid phase. The case where $\{Fe^{3+}\} > K_S\{OH^-\}^{-3}$ is thermodynamically impossible at equilibrium, but is frequently observed in metastable "oversaturated" solutions.

Although this approach generally works well, it suffers from several problems:

1. Solids are able to interact with species in solution in ways other than just by equal exchange of the ions that comprise the solid. Thus there exists an ill-defined transition between the ideal behaviour of dissolved and solid-phase species which is currently dealt with by invoking adsorption and surface precipitation phenomena.
2. The solubility product has been observed to vary with precipitate surface area, e.g. for precipitates of thorium (Fanghänel and Neck, 2002). This can again be explained by invoking surface-mediated phenomena, but is clearly inconsistent with a strict interpretation of a solubility product.
3. It is mechanistically difficult to reconcile this result with the dynamics of actual chemical processes.

We will address the final issue in the following sections, and aim to demonstrate that a polymer-based model is more mechanistically consistent than the existing thermodynamic approach (although it is certainly not perfect). We will then proceed in the final sections of this paper to show how a polymer-based model provides a more unified approach to the treatment of dissolved and solid-phase species, thus helping to address the first two issues associated with the conventional thermodynamic approach.

2.3. Reaction mechanism for iron precipitation

Precipitation can proceed either via the reaction of two dissolved species to form a solid (homogeneous precipitation), or the reaction of a dissolved species with an existing solid (heterogeneous precipitation). Stumm (1992) described the process of precipitation as occurring in three steps:

1. The formation of small oligomers from the interaction of dissolved molecules leading to formation of a polynuclear complex of some critical size (nucleus):

$$X + X \rightleftharpoons X_2$$
$$X + X_2 \rightleftharpoons X_3$$
$$\vdots$$
$$X + X_{j-1} \rightleftharpoons X_j \text{ (nucleus)}$$

(In the case of heterogeneous precipitation this step may not occur, since nuclei already exist.)

2. Deposition of more material on the nuclei by further polymerisation to form small, solid crystallites:

$$X + X_j \rightarrow \text{crystallite}$$
$$X + \text{crystallite} \rightarrow \text{larger crystallite}$$

3. Formation of large crystals from small crystallites by aggregation and ripening.

The homogeneous precipitation of iron(III) in solution is initiated by hydrolysis (Eqs. (1)–(6)). Hydrolysed monomeric species (Fe′) can undergo polymerisation reactions, initially forming oligomeric polynuclear complexes which can then undergo further polymerisation to form large-chain polymers and, at some point, solid-phase structures (Dousma and De Bruyn, 1976). Iron(III) exhibits octahedral coordination in monomeric and polymeric forms under the vast majority of environmental conditions (Combes et al., 1989; Cornell and Schwertmann, 2004). The formation of dimers (and probably other oligomers during initiation of precipitation) occurs through olation reactions in which Fe atoms share bridging hydroxide ligands:

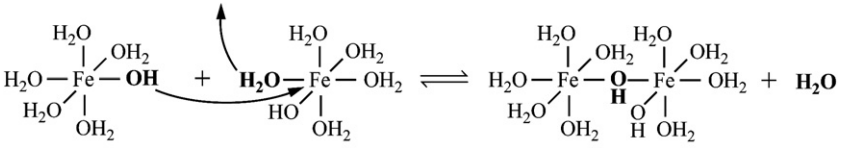

(9)

The rate of olation reactions is typically limited by the rate at which the coordinated water molecule is expelled (Jolivet et al., 2006). Olation is usually relatively fast (Jolivet et al., 2006), and the reaction is readily reversible (Blesa and Matijević, 1989). The reaction in Eq. (9) involves formation of a single hydroxy-bridge, leading to corner-sharing between the octahedra for each Fe atom. However Fe(III) oligomers typically involve considerable amounts of edge-sharing between octahedra, corresponding to a double hydroxy-bridge. Such bonding has been established for the well-studied $[Fe_2(OH)_2(OH_2)_8]^{4+}$ dimer (Sommer and Margerum, 1970), which forms through the reaction of two $[Fe(OH)(OH_2)_5]^{2+}$ monomers at low pH:

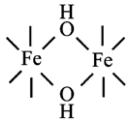

The existence of such bonding arrangements has also been well established on the basis of X-ray spectroscopy for larger oligomers (Rose et al., 1997a), although primarily at low pH and high Fe(III) concentrations.

The second major type of iron(III) polymerisation reaction is oxolation, which involves sharing of oxygen bridging ligands between Fe atoms. Formation of oxy-bridges between Fe atoms requires dehydration of an existing hydroxy-bridge, and must therefore occur in two steps (Jolivet et al., 2006). The reaction involves condensation of two hydroxide ligands to release a water molecule, not simply deprotonation of a single hydroxide ligand (Flynn, 1984; Jolivet et al., 2006). Consequently oxolation reactions are slower than olation reactions (Flynn, 1984), and appear to be difficult to reverse (Blesa and Matijević, 1989).

A considerable amount of work has been done to elucidate the precise mechanism(s) involved in the initial steps of iron(III) precipitation, particularly using X-ray absorption techniques such as XANES (X-ray absorption near edge structures), EXAFS (extended X-ray absorption fine structures), WAXS (wide angle X-ray scattering) and SAXS (small-angle X-ray scattering) to provide detailed structural information about the precursor species for nucleation and crystal formation (Combes et al., 1989; Bottero et al., 1994; Rose et al., 1996, 1997a,b). At relatively low pH values, and in the presence of particular anions, it appears that nuclei with a specific size and structure may form via a series of well-characterised steps. For example, a 0.1 M $FeCl_3$ solution will initially form a dimer, subsequently adding another monomeric Fe(III) species to form a trimer, of which eight will bond to form an oligomeric nucleus containing 24 Fe atoms in a regular arrangement (Bottero et al., 1994). These nuclei then aggregate to produce crystallites with well-defined structures such as akaganéite (Bottero et al., 1994; Cornell and Schwertmann, 2004).

However, at pH values above about 3 the process of Fe(III) precipitation is chaotic (Rose et al., 1997a). In any case, the initial formation of small dimers and oligomers, and subsequently of larger polymers, proceeds primarily via olation reactions and consequently is easily reversible (Dousma and De Bruyn, 1976). As large polymers develop, simultaneously-occurring oxolation reactions produce stronger bonding between Fe atoms and result in much slower depolymerisation (Dousma and De Bruyn, 1976). Eventually these large polymers transition from being dissolved to non-dissolved species and the process of precipitation occurs.

2.4. Reaction mechanism for iron dissolution

Depolymerisation (dissolution) proceeds in the absence of light, organic ligands or reductants via weakening of bonds between Fe atoms in the polymer due to the reaction of these Fe atoms with protons and/or water molecules

(Zinder et al., 1986; Stumm, 1992; Cornell and Schwertmann, 2004). Dissolution of FOP species proceeds via the sequential loss of one Fe atom as hydroxy- and oxy-bridging ligands between the atom and its neighbours are protonated (Zinder et al., 1986). Typically only one Fe atom is detached at a time, because detachment of one Fe atom from a polymer requires the weakening of at most five bonds (and almost certainly far less than this in a fractal structure), whereas detachment of multiple Fe atoms as a smaller polymer would require the almost simultaneous weakening of multiple bonds between multiple Fe atoms.

3. POLYMER-BASED MODEL

3.1. Polymerisation and precipitation

Polymerisation of iron(III) can hypothetically occur through the reaction of any monomeric iron(III) species with any other iron(III) species, monomeric or otherwise. We can write this series of polymerisation reactions as:

$$\mathrm{Fe}_i + \mathrm{Fe}_j \xrightarrow{k_{fij}} \mathrm{Fe}_{(i+j)} \tag{10}$$

where Fe_i and Fe_j represent any iron(III) species (monomeric or otherwise), $\mathrm{Fe}_{(i+j)}$ is the resulting FOP species consisting of $(i+j)$ Fe atoms, and k_{fij} is the corresponding second-order rate constant for the reaction.

Although polymerisation reactions involving two oligomers or polymers may be important determinants of the form of FOP at any given time, mechanistic studies indicate that the primary reactions that initially occur during homogeneous Fe(III) precipitation at pH > 3 are chaotic olation reactions leading to fractal structures (Rose et al., 1997a). The fractal dimension of Fe(III) polymers appears to increase with increasing [OH$^-$]:[Fe(III)] ratio (Bottero et al., 1991; Tchoubar et al., 1991), indicating a shift from linear structures to semi-linear structures as this ratio increases. Higher fractal dimensions suggest dominance of a particle–cluster mode of polymer growth rather than a cluster–cluster mode of growth (Meakin, 1984). Although the fractal dimension of 1.75 observed by Bottero et al. (1991) at the highest examined [OH$^-$]:[Fe(III)] ratio of 2.8 appeared to conform to a cluster–cluster mode of growth, the [OH$^-$]:[Fe(III)] ratio was still considerably less than what might be expected at circumneutral pH. This suggests that Fe(III) polymerisation at pH > 3, where [OH$^-$]:[Fe(III)] ratios are higher still, probably proceeds mostly via the addition of Fe′ to existing oligomers or, initially, to other Fe′ molecules, rather than by the aggregation of oligomers. Although we use this argument as the basis for constructing our model in this work, we note that the issue has not been resolved experimentally. As will be seen in the subsequent development of the model, this would not be expected to significantly influence the rate of loss of Fe′ from solution due to polymerisation, but would almost certainly influence the rate of depolymerisation (dissolution) and the size distribution of polymers as a function of time. Incorporating cluster–cluster growth into the model was beyond our capabilities mathematically, but deserves attention in future modelling attempts.

Thus, subject to this important caveat, we will neglect reactions between oligomers at this stage and examine only the fate of Fe′. Eq. (10) then simplifies to:

$$\mathrm{Fe}_i + \mathrm{Fe}' \xrightarrow{k_{fi}} \mathrm{Fe}_{i+1} \tag{11}$$

where Fe_i again represents any iron(III) species (monomeric or otherwise), Fe_{i+1} is the resulting FOP species consisting of $(i+1)$ Fe atoms in an unspecified arrangement, and k_{fi} is the second-order rate constant for the reaction.

In the pH range 6.5–9.0, at least at relatively high [OH$^-$]:[Fe(III)] ratios, Fe′ polymerisation is governed by reaction of the dissolved neutral species $\mathrm{Fe(OH)}^0_{3(aq)}$ (Pham et al., 2006). This is because the rate-limiting step for olation tends to be the loss of the first water molecule from the collision of two reacting species, and the water exchange kinetics of $\mathrm{Fe(OH)}^0_{3(aq)}$ are extremely rapid compared to other hydrolysed iron(III) species (Eigen and Wilkins, 1965; Blesa and Matijević, 1989). At pH values outside this range, the kinetics of polymerisation could instead be governed by the slower water exchange kinetics of the less hydrolysed monomeric species, such as $\mathrm{Fe(H_2O)}_6^{3+}$, $\mathrm{Fe(H_2O)_5\ (OH)}^{2+}$ and $\mathrm{Fe(H_2O)_4(OH)}_2^{+}$. However, it has been shown that the precipitation rate is proportional to the $\mathrm{Fe(OH)}^0_{3(aq)}$ concentration even at pH values below 3 (Grundl and Delwiche, 1993), and it has been suggested that this species controls the kinetics of Fe(III) precipitation at all pH values (Jolivet et al., 2006).

The rate constant for this reaction, k_{fi}, is related to both the collision frequency of a molecule of Fe′ with a molecule of Fe_i and a steric factor that reflects the probability that the collision will occur in such a way that the incoming Fe′ molecule can successfully bond to the Fe_i molecule. Flory (1946) argued that the steric factors affecting a particular atom (or basic molecular unit) within a polymer are dominated entirely by factors in the local environment of the atom, and are unaffected by polymer-scale factors (such as the rate of diffusion of the whole molecule, or the precise arrangement of atoms within the polymer). Thus, reactions of a particular atom can be treated independently of any other atom except to the extent that its local coordination environment is affected (i.e. an existing bond with an atom will clearly prevent bonding of another atom at that coordination site). Subsequent work has confirmed that the Flory principle holds for all but a few "non-ideal" polymers, namely those in which occupation of one coordination site affects the coordinative properties of other sites on an atom or molecule (short-range effects), or those in which the interaction of the polymer with the solvent inhibits its accessibility of the coordination sites (long-range effects) (Kuchanov et al., 2004). The Flory principle also neglects intramolecular reactions (Flory, 1946; Kuchanov et al., 2004).

We would expect that FOP would behave at least initially as an ideal polymer, and therefore conform to the Flory principle. Although it may seem that long-range non-ideal effects occur during formation of highly crystalline polymers, these effects are better considered as saturation of coordination sites on a Fe atom rather than shielding of atoms from the solvent water. Additionally, although intramolecular reactions are important (most

notably the condensation of hydroxy-bridges to oxy-bridges), it is reasonable to expect that such reactions will not influence polymerisation processes, given that the rate of these processes is governed by the rate of water loss from incoming Fe′ rather than the coordinative environment of Fe atoms in the polymer.

Applying the Flory principle, assuming that $Fe(OH)^0_{3(aq)}$ is in equilibrium with other monomeric Fe′ species, and making an initial approximation that all Fe atoms have at least one available coordination site, leads to the relationship:

$$k_{fi} = i\alpha_{Fe(OH)^0_3} k_f \tag{12}$$

where $\alpha_{Fe(OH)^0_3}$ is the proportion of Fe′ that is $Fe(OH)^0_3$ at a specified pH, and $k_f = 2.0 \times 10^7\ M^{-1}\ s^{-1}$ is the second-order rate constant for reaction of $Fe(OH)^0_{3(aq)}$ with Fe atoms in either Fe′ or a polymer at 25 °C in 2 mM $NaHCO_3$ and 10 mM NaCl (Pham et al., 2006). The approximation that all Fe atoms can react with Fe′ should be a good one initially in systems where chaotic olation is dominant since the polymers thus formed possess amorphous, fractal structures with relatively two-dimensional character (Rose et al., 1997a). However the approximation will begin to fail as the polymer becomes increasingly ordered over time. This issue will be addressed further when we apply the model to existing observations in later sections.

Under these conditions, the rate of polymerisation of Fe′ is thus given by:

$$\begin{aligned} -\frac{d}{dt}[Fe'] &= \alpha_{Fe(OH)^0_3} k_f [Fe'](2[Fe'] + 2[Fe_2] + 3[Fe_3] \\ &\quad + 4[Fe_4] + \cdots + (n-1)[Fe_{n-1}]) \\ &= \alpha_{Fe(OH)^0_3} k_f [Fe'] \left([Fe'] - n[Fe_n] + \sum_{i=1}^{n} i[Fe_i] \right) \\ &= k_f^* [Fe']^2 + k_f^* [Fe'][Fe]_T - n k_f^* [Fe'][Fe_n] \end{aligned} \tag{13}$$

where k_f^* is a conditional second-order rate constant at a particular pH, n is the number of Fe atoms in the largest polymer that can form, and $[Fe]_T$ represents the total concentration of Fe atoms in the system. Note that the coefficient of $[Fe']$ is 2, as the reaction of Fe′ with Fe′ results in removal of twice as many Fe′ molecules at a time as does the reaction of Fe′ with other polymers, and there is no reaction of Fe′ with Fe_n, as Fe_n is the largest possible polymer that can form. It is also possible to formulate Eq. (13) as an infinite sum, in which case the results we derive in the following sections still follow, however the reasoning is simpler with a finite number of possible polymers. This formulation is also more realistic, as the maximum polymer size in a system is clearly limited by the number of Fe atoms in the system.

3.2. Depolymerisation and dissolution

Since FOP dissolution proceeds via the detachment of Fe atoms from the polymer one at a time, we can write the reaction for dissolution as the reverse of Eq. (11):

$$Fe_{i+1} \xrightarrow{k_{di+1}} Fe_i + Fe' \tag{14}$$

where Fe_{i+1} is a FOP species consisting of $(i+1)$ Fe atoms, Fe_i is either a FOP species consisting of i Fe atoms (if $i > 1$) or Fe′ (if $i = 1$), and k_{di+1} is the first-order rate constant for dissolution of the FOP species.

Unlike polymerisation, whose rate depends primarily on a fundamental chemical property of a single dissolved species, depolymerisation (dissolution) kinetics depends strongly on the nature of the polymerised atom(s). For example, depolymerisation of a Fe atom coordinated to the polymer by only corner-sharing requires breaking only a single bond, whereas depolymerisation of a Fe atom coordinated by edge-sharing requires breaking of two bonds. Furthermore, the strength of each bond will be affected by the type of bond (hydroxy-bridge versus oxy-bridge) and the distribution of electron density around a particular Fe atom due to the type and number of bonds. If we assume that the former factor is dominant, then the rate of dissolution will be a first-order process for Fe atoms in each possible type of bonding arrangement. Assuming further that every polymer of the same size will contain the same number of Fe atoms in each type of coordination environment, and that depolymerisation of all Fe atoms with the same type of coordination environment proceeds with the same rate constant, we can express the rate law for depolymerisation in terms of liberation of Fe′ as:

$$\begin{aligned} \frac{d}{dt}[Fe'] &= \sum_{\text{all } x \text{ and } y} k_{dx,y} [Fe(x,y)]_T \\ &= \sum_{\text{all } x \text{ and } y} \left(k_{dx,y} \sum_{i=2}^{n} [Fe(x,y)_i] \right) \\ &= \sum_{\text{all } x \text{ and } y} \sum_{i=2}^{n} k_{dx,y} \alpha_{Fe(x,y)_i} i [Fe_i] \\ &= \sum_{i=2}^{n} [Fe_i] i \sum_{\text{all } x \text{ and } y} k_{dx,y} \alpha_{Fe(x,y)_i} \end{aligned} \tag{15}$$

where $[Fe(x,y)_i]$ represents the concentration of Fe atoms coordinated by x hydroxy-bridges and y oxy-bridges in a polymer with i Fe atoms in total, $[Fe(x,y)]_T$ represents the total concentration of such atoms in the system, $k_{dx,y}$ is the rate constant for depolymerisation of such an atom, and $\alpha_{Fe(x,y)_i}$ is the proportion of atoms in polymer Fe_i in such a coordination state.

This type of formulation corresponds to the sum of the rate laws generated from the series of reactions represented in Eq. (14), where

$$k_{di} = i \sum_{\text{all } x \text{ and } y} k_{dx,y} \alpha_{Fe(x,y)_i} \tag{16}$$

In reality, the rate of dark, thermal, non-reductive dissolution of Fe(III) solids is not a simple first-order process (Cornell and Schwertmann, 2004). However, on sufficiently short timescales the rate of depolymerisation appears to be described well by a process that is first-order in the total concentration of Fe atoms in FOP for most types of polymeric and/or solid phase Fe(III) (Kuma et al., 1992, 1993; Rose and Waite, 2003). This is mechanistically plausible in the context of our model provided that the values of $\alpha_{Fe(x,y)_i}$ remain relatively constant on the timescale of

interest. During a homogeneous precipitation process, we would initially expect values of $\alpha_{Fe(x,0)_i}$ to be highest, but as time progresses we would expect to see values of $\alpha_{Fe(x,y)_i}$ corresponding to fully coordinated Fe atoms and to coordination environments involving oxy-bridges increase. Consequently, the apparent rate constants k_{di} will decrease over time.

Thus we can write a first-order rate law for depolymerisation (expressed as liberation of Fe′):

$$\frac{d}{dt}[Fe'] = 2k_{d2}[Fe_2] + k_{d3}[Fe_3] + k_{d4}[Fe_4] + \cdots + k_{dn}[Fe_n] \quad (17)$$

where k_{di} is a first-order rate constant for the detachment of a Fe atom from a polymer Fe_i that consists of Fe atoms in a typical bonding arrangement at a particular time and at a particular pH. As with Eq. (13), the coefficient of $[Fe_2]$ is twice that of the other polymers, since depolymerisation of Fe_2 will yield two Fe′ molecules (compared with only one Fe′ molecule for depolymerisation of any other polymer), and again we have a finite number of polymers that can possibly form.

In a further simplification still, it may be possible over sufficiently short time periods to assume that the values of $\alpha_{Fe(x,y)_i}$ are independent of i, such that values of $k_{di}/i = k_d^*$ (a constant) for all i. From the perspective of a conventional surface chemistry approach, this is equivalent to a condition in which the concentration of particular surface species is proportional to the surface area (Stumm, 1997), which is in turn considered to be proportional to the total concentration of Fe atoms. This latter condition is typically true in systems containing substantial amounts of precipitate over a timescale where the particle size distribution does not change significantly. We would also expect this condition to hold for highly amorphous polymers (e.g. in the initial stages of homogeneous precipitation), in which case all atoms are effectively surface species. This leads to the equation:

$$\begin{aligned}\frac{d}{dt}[Fe'] &= 2k_d^*2[Fe_2] + k_d^*3[Fe_3] + k_d^*4[Fe_4] + \cdots + k_d^*n[Fe_n] \\ &= 2k_d^*[Fe_2] - k_d^*[Fe'] + k_d^*[Fe]_T \end{aligned} \quad (18)$$

where k_d^* is a conditional first-order rate constant at a particular pH and for a particular distribution of Fe bonding arrangements, and $[Fe]_T$ is the concentration of the total number of Fe atoms in the system. Note that the key difference between Eqs. (17) and (18) is that the former is in terms of the concentration of molecules of each polymer, which necessitates the use of individual rate constants k_{di}, while the latter is in terms of the concentration of Fe atoms in each polymer.

In a system in which a substantial amount of precipitate is present, only the final term in Eq. (18) is significant and the equation reduces to:

$$\frac{d}{dt}[Fe'] = k_d^*[Fe]_T \quad (19)$$

Such an approach has been shown to be valid for dissolution of two well-characterised Fe solid-phases, colloidal hydrous ferric oxide (Kuma et al., 1992) and colloidal lepidocrocite (Kuma et al., 1993), in seawater at a range of circumneutral pH values, as well as freshly precipitated amorphous Fe(III) in seawater at pH 8.1 (Rose and Waite, 2003). This work indicates that a single value for k_d^* is valid on a timescale of at most tens of minutes for freshly precipitated material, however this material dissolves on a timescale of seconds to minutes (Rose and Waite, 2003). As the precipitate ages the value of k_d^* decreases, but so too does the rate at which k_d^* changes. For example, the timescale of dissolution for material that is 24 h old increases to several hours, but the value of k_d^* is relatively constant on a timescale of around 12 h (Rose and Waite, 2003). Similarly, a single value of k_d^* is valid for at least several days in the case of precipitated material that is one week old (Kuma et al., 1992, 1993). Interpolating these observations, it would seem that the timescale for significant change in the value of k_d^* is in general greater by a factor of at least 2–3 than the timescale of dissolution. In all cases, the timescale for polymerisation reactions is considerably shorter than for depolymerisation. Thus it appears reasonable to consider pseudo-equilibrium on timescales of around 10–15 min for freshly precipitated material, and up to several days for material that is at least one week old.

4. APPLICATION OF THE POLYMER-BASED MODEL TO THE CONCEPT OF A SOLUBILITY LIMIT

4.1. Theoretical relationship

4.1.1. Approach 1: Fe solubility assuming single rate constants for precipitation and dissolution when only Fe′ is considered dissolved

Based on the rate laws for Fe(III) polymerisation and depolymerisation in Eqs. (13) and (18), we can write an overall rate law for Fe′:

$$\begin{aligned}\frac{d}{dt}[Fe'] &= 2k_d^*[Fe_2] - k_d^*[Fe'] + k_d^*[Fe]_T - k_f^*[Fe']^2 \\ &\quad - k_f^*[Fe'][Fe]_T + nk_f^*[Fe'][Fe_n] \end{aligned} \quad (20)$$

Similarly, we can obtain rate laws for each of the polymeric species:

$$\begin{aligned}\frac{d}{dt}[Fe_i] &= (i-1)k_f^*[Fe'][Fe_{i-1}] - ik_d^*[Fe_i] - ik_f^*[Fe'][Fe_i] \\ &\quad + (i+1)k_d^*[Fe_{i+1}] \end{aligned} \quad (21)$$

Provided that we meet the conditions for k_d^* and k_f^* to remain constant (i.e. constant pH and a constant distribution of Fe bonding arrangements in the system), then the system will reach a pseudo-equilibrium where the forward and backwards rates of each polymerisation/depolymerisation reaction are equal and the overall rate of change of the Fe′ concentration is zero. Expressing this condition for each polymer of size $\geqslant i$ Fe atoms, summing for all equations generated thus, and substituting to express the result in terms of Fe′ only gives the relationship:

$$[Fe_i] = \frac{1}{i}\left(\frac{k_f^*[Fe']}{k_d^*}\right)^{i-1}[Fe'] \quad (22)$$

Full details of this derivation are provided in Electronic Annex EA-1.

Now substituting the expressions for $[Fe_2]$ and $[Fe_n]$ from Eq. (22) into Eq. (20) at equilibrium gives:

$$\frac{d}{dt}[Fe'] = k_f^*[Fe']^2 - k_d^*[Fe'] + k_d^*[Fe]_T - k_f^*[Fe']^2 - k_f^*[Fe'][Fe]_T + k_f^*[Fe']^2\left(\frac{k_f^*[Fe']}{k_d^*}\right)^{n-1} \quad (23)$$

i.e. $$k_d^*[Fe]_T - (k_f^*[Fe]_T + k_d^*)[Fe'] + k_f^*[Fe']^2\left(\frac{k_f^*[Fe']}{k_d^*}\right)^{n-1} = 0 \quad (24)$$

Provided that $[Fe'] < k_d^*/k_f^*$, the final term approaches zero as $n \to \infty$, giving:

$$[Fe'] = \frac{k_d^*[Fe]_T}{k_f^*[Fe]_T + k_d^*} \quad (25)$$

The relationship in Eq. (25) is hyperbolic, with asymptotes of $[Fe'] = [Fe]_T$ when $[Fe]_T \ll k_d^*/k_f^*$, and $[Fe'] = k_d^*/k_f^*$ when $[Fe]_T \gg k_d^*/k_f^*$, as shown in Fig. 2 using typical values of $k_f^* = 10^7\ M^{-1}\ s^{-1}$ and $k_d^* = 10^{-5}\ s^{-1}$. This is consistent with the notion of a solubility limit insofar as there is some finite value (k_d^*/k_f^*) for the maximum solubility of iron above which the $[Fe']$ is constant, and below which all iron is present as Fe′. The relationship is not identical to what we expect from the traditional definition of solubility: the hyperbola is curved around the solubility limit of k_d^*/k_f^*, so that there is a range of values of $[Fe]_T$ near but less than k_d^*/k_f^* in which some precipitation occurs. In the traditional interpretation of a solubility limit, there should be strictly no precipitation until the solubility limit is reached.

There is, to our knowledge, no experimental evidence that the real solubility behaviour of iron(III) (or indeed any ion) is as sharply defined as the traditional solubility limit concept, and the curvature of the hyperbola would be difficult to distinguish experimentally due to the very low iron(III) concentrations involved.

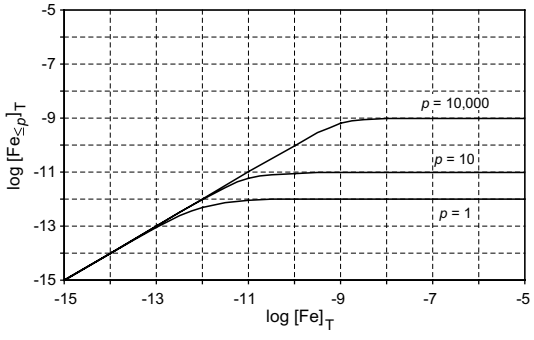

Fig. 2. Prediction of a solubility limit relationship using the polymer-based model using either Approach 1 (single rate constants for precipitation and dissolution) or Approach 3 (multiple rate constants for precipitation and dissolution with the same ratio) as simplifying assumptions to the series of rate law equations. Simulations are shown assuming that only Fe′ is considered dissolved ($p = 1$) or that all polymers containing no more than 10 ($p = 10$) or 10^4 ($p = 10{,}000$) Fe atoms are considered dissolved. Typical values of $k_f^* = 10^7\ M^{-1}\ s^{-1}$ and $k_d^* = 10^{-5}\ s^{-1}$ (Approach 1) or $K^* = 10^{12}\ M^{-1}$ (Approach 3), yielding equivalent results, were used.

4.1.2. Approach 2: Fe solubility assuming different rate constants for homogeneous and heterogeneous precipitation when only Fe′ is considered dissolved

Another possibility may be that the assumptions used in derivation of the model contribute to the observed curvature around the solubility limit. An obvious problem lies within the requirement for constant values of k_f^* and k_d^*, namely that while it may be reasonable to assume similar bonding arrangements in larger polymers, it is a very crude approximation to assume that Fe′, in which all coordination sites for polymerisation are vacant, will possess similar bonding arrangements to larger polymers. We can improve this approximation by assuming instead that there are two values for $k_f^* : k_{f1}^*$, which applies to the homogeneous polymerisation reaction of Fe′ with Fe′, and $k_{f2\to n}^*$, which applies to heterogeneous polymerisation reactions of Fe′ with FOP. In this case, Eq. (13) becomes:

$$-\frac{d}{dt}[Fe'] = (2k_{f1}^* - k_{f2\to n}^*)[Fe']^2 + k_{f2\to n}^*[Fe'][Fe]_T - nk_{f2\to n}^*[Fe'][Fe_n] \quad (26)$$

Eq. (18) is unchanged, and Eq. (24) will become:

$$(k_{f2\to n}^* - k_{f1}^*)[Fe']^2 - (k_{f2\to n}^*[Fe]_T + k_d^*)[Fe'] + k_d^*[Fe]_T + k_{f2\to n}^*[Fe']^2\left(\frac{k_{f1}^*[Fe']}{k_d^*}\right)\left(\frac{k_{f2\to n}^*[Fe']}{k_d^*}\right)^{n-2} = 0 \quad (27)$$

(see Electronic Annex EA-1 for detailed derivation).

Again as $n \to \infty$, provided that $[Fe'] < k_d^*/k_{f2\to n}^*$ the final term approaches zero, yielding the quadratic equation:

$$(k_{f2\to n}^* - k_{f1}^*)[Fe']^2 - (k_{f2\to n}^*[Fe]_T + k_d^*)[Fe'] + k_d^*[Fe]_T = 0 \quad (28)$$

whose solution is given by:

$$[Fe'] = \frac{k_{f2\to n}^*[Fe]_T + k_d^* \pm \sqrt{(k_{f2\to n}^*[Fe]_T - k_d^*)^2 + 4k_{f1}^*k_d^*[Fe]_T}}{2(k_{f2\to n}^* - k_{f1}^*)} \quad (29)$$

As $k_{f1}^* \to 0$, the solution to Eq. (28) simplifies further to:

$$[Fe'] = \frac{k_{f2\to n}^*[Fe]_T + k_d^* \pm (k_{f2\to n}^*[Fe]_T - k_d^*)}{2k_{f2\to n}^*} = \begin{cases} [Fe]_T, & [Fe]_T \leqslant k_d^*/k_{f2\to n}^* \\ k_d^*/k_{f2\to n}^*, & [Fe]_T > k_d^*/k_{f2\to n}^* \end{cases} \quad (30)$$

which corresponds exactly to the thermodynamic expression of a solubility limit. However, it is difficult to envisage circumstances in which k_{f1}^* would ever be less than $k_{f2\to n}^*$, let alone approach zero, given that the only difference between the rate constants should arise from availability of coordination sites (the other governing factor, the rate of water loss from $Fe(OH)^0_{3(aq)}$, will be the same in both cases). In fact it seems more likely that k_{f1}^* should always be greater than $k_{f2\to n}^*$, which leads to an even greater degree of curvature around the solubility limit than is predicted in the case

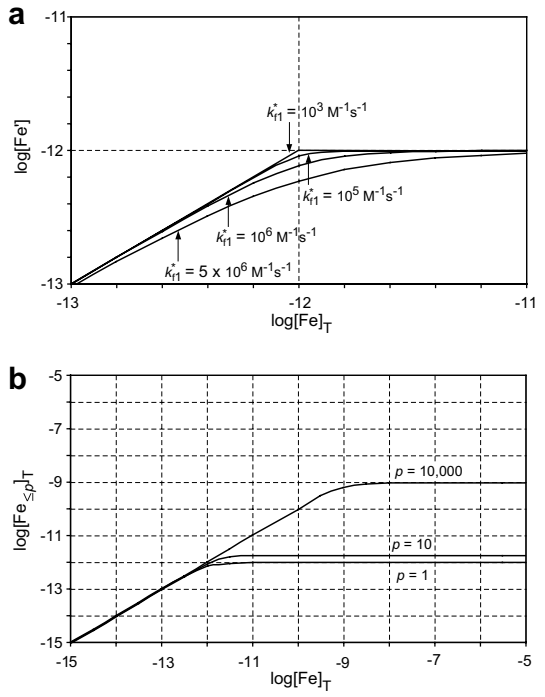

Fig. 3. Prediction of a solubility limit relationship using the polymer-based model using Approach 2 (two different rate constants for homogeneous and heterogeneous precipitation and a single rate constant for dissolution). (a) Effect of varying k^*_{f1} on the predicted [Fe′] using values of $k^*_{f2\to n} = 10^7\ M^{-1}\ s^{-1}$ and $k^*_d = 10^{-5}\ s^{-1}$. (b) Empirically-derived solubility limit relationship assuming that only Fe′ is considered dissolved ($p = 1$) or that all polymers containing no more than 10 ($p = 10$) or 10^4 ($p = 10{,}000$) Fe atoms are considered dissolved when $k^*_{f1} = 10^6\ M^{-1}\ s^{-1}$, $k^*_{f2\to n} = 10^7\ M^{-1}\ s^{-1}$ and $k^*_d = 10^{-5}\ s^{-1}$.

that $k^*_{f1} = k^*_{f2\to n} = k^*_f$. Solubility relationship simulations using this approach as k^*_{f1} is varied are shown in Fig. 3(a) using typical (constant) values of $k^*_{f2\to n} = 10^7\ M^{-1}\ s^{-1}$ and $k^*_d = 10^{-5}\ s^{-1}$.

4.1.3. Approach 3: Fe solubility assuming multiple rate constants for precipitation and dissolution when only Fe′ is considered dissolved

Although an approach considering different rate constants for homogeneous and heterogeneous precipitation is more reasonable than the initial approach using only one rate constant, it is still a somewhat crude approximation. In the previous approach, we have considered a heterogeneous reaction of Fe′ with a dimer to occur with the same rate constant as the heterogeneous reaction of Fe′ with a large polymer, whereas in reality the rate constant for the heterogeneous reaction of Fe′ with a dimer would probably be closer to that of the homogeneous reaction. The generality of this approach can be improved further by assuming that the rate constants for each of the reactions of Fe′ with any other Fe species are independent of one another. As stated, the only difference between these rate constants should arise from decreasing availability of coordination sites with larger polymers. As this factor should similarly affect the rate constants for dissolution of each species, we will assume that while the individual k^*_{fi} and k^*_{di} vary, the ratio $K^* = \frac{k^*_{fi}}{k^*_{di}}$ remains constant on a timescale of pseudo-equilibrium.

Consequently, the form of Eq. (22) becomes:

$$[Fe_i] = \frac{1}{i}[Fe']\left(\prod_{j=2}^{i}\frac{k^*_{f(j-1)}}{k^*_{dj}}[Fe']\right) \tag{31}$$

(see Electronic Annex EA-1 for detailed derivation). If we further assume that $k^*_{f(j-1)} \approx k^*_{fj}$, this simplifies to:

$$[Fe_i] = \frac{1}{i}[Fe']\left(\prod_{j=2}^{i}K^*[Fe']\right) = \frac{1}{i}[Fe'](K^*[Fe'])^{i-1} \tag{32}$$

which is essentially the same as Eq. (22), leading to a hyperbolic solubility relationship similar to Eq. (25):

$$[Fe'] = \frac{[Fe]_T}{K^*[Fe]_T + 1} \tag{33}$$

(full details of the derivation are provided in Electronic Annex EA-1). Note that the notation $k^*_{f(j-1)} \approx k^*_{fj}$ is rather mathematically informal and does not imply that $k^*_{f1} \approx k^*_{f2} \approx \cdots \approx k^*_{fj} \approx \cdots \approx k^*_{fn-1} \approx k^*_{fn}$, in which case this approach would be identical to the first approach. This approach is also represented in Fig. 2, using a typical value of $K^* = 10^{12}\ M^{-1}$.

4.1.4. Solubility of Fe when small oligomers are also considered dissolved

The three approaches presented all result in prediction of an upper limit on the Fe′ concentration, consistent with the notion of a solubility limit. However, solubility measurements based on filtration probably capture small polymers in addition to Fe′. We therefore now extend our analysis to consider the equilibrium concentration of all oligomers containing less than a certain number, p, of Fe atoms, which would correspond more closely to solubility measurements based on molecular size.

Under the first approach (only one rate constant for precipitation, k^*_f), from Eq. (22) the concentration of Fe atoms either as Fe′ or in polymers containing at most p atoms is given by:

$$\begin{aligned}[Fe_{\leqslant p}]_T &= \sum_{i=1}^{p} i[Fe_i] = [Fe']\sum_{i=0}^{p-1}\left(\frac{k^*_f[Fe']}{k^*_d}\right)^i \\ &= [Fe']\frac{1-(k^*_f[Fe']/k^*_d)^p}{1-(k^*_f[Fe']/k^*_d)}\end{aligned} \tag{34}$$

Rearranging Eq. (25) in terms of $[Fe]_T$ and substituting gives:

$$\begin{aligned}[Fe_{\leqslant p}]_T &= [Fe]_T(1-(k^*_f[Fe']/k^*_d)^p) \\ &= [Fe]_T\left(1-\left(\frac{[Fe]_T}{[Fe]_T + k^*_d/k^*_f}\right)^p\right)\end{aligned} \tag{35}$$

Although it is not as obvious as for Eq. (25), this equation defines a similar relationship to Eq. (25) except that the solubility limit is higher by a factor of p, i.e. when $[Fe]_T \gg pk^*_d/k^*_f$, $[Fe_{\leqslant p}]_T \approx pk^*_d/k^*_f$ and when $[Fe]_T \ll pk^*_d/k^*_f$, $[Fe_{\leqslant p}]_T \approx [Fe]_T$ (see Electronic Annex EA-1 for details). The effect of consider-

ing different values of p as defining dissolved versus non-dissolved Fe on solubility simulations using Approach 1 is shown in Fig. 2. Although the apparent value of the solubility limit increases when we increase the fraction of polymers that are considered to be dissolved, the curvature near where $[Fe]_T$ approaches the solubility limit still exists. Thus the deviation from the conventional concept of a solubility limit does not appear to be due to what polymer sizes are considered to be dissolved.

A similar relationship is derived in the case of the third approach, where the concentration of Fe atoms either as Fe′ or in polymers containing at most p atoms is given by:

$$[Fe_{\leqslant p}]_T = [Fe'] \sum_{i=0}^{p-1} (K^*[Fe'])^i = [Fe'] \frac{1-(K^*[Fe'])^p}{1-K^*[Fe']} = [Fe]_T \left(1 - \left(\frac{[Fe]_T}{[Fe]_T + 1/K^*}\right)^p\right) \quad (36)$$

which clearly possesses similar properties to Eq. (35). The effect of considering different values of p as defining dissolved versus non-dissolved Fe on solubility simulations using Approach 3 is also shown in Fig. 2.

For the second approach, the relationship is considerably more complicated although, again, some form of solubility limit is predicted. In this case, we obtain the sum:

$$[Fe_{\leqslant p}]_T = \sum_{i=1}^{p} i[Fe_i] = [Fe'] + \sum_{i=2}^{p} \frac{k_{f1}^*}{k_d^*}[Fe']^2 \left(\frac{k_{f2\to n}^*[Fe']}{k_d^*}\right)^{i-2} = [Fe'] \frac{1+(k_{f1}^* - k_{f2\to n}^*)[Fe']/k_d^* - k_{f1}^*/k_{f2\to n}^*(k_{f2\to n}^*[Fe']/k_d^*)^p}{1-(k_{f2\to n}^*[Fe']/k_d^*)} \quad (37)$$

The situation of most interest is when $k_{f1}^* \to 0$, in which case Eq. (37) simplifies to $[Fe_{\leqslant p}]_T = [Fe']$; i.e. any Fe that is not Fe′ exists as a single, large polymer. Again, this relationship is the most consistent with the conventional concept of a solubility limit, but is quite inconsistent with the range of polymers of various sizes (both dissolved and non-dissolved) that are observed in reality. When $k_{f1}^* > 0$, Eq. (37) empirically appears to predict a solubility limit relationship, however there is no obvious mathematical simplification that demonstrates this limiting behaviour. The effect of considering different values of p as defining dissolved versus non-dissolved Fe on solubility simulations using Approach 2 is shown in Fig. 3(b).

4.1.5. Comparison of approaches

A common feature of all approaches is the prediction of a solubility limit, despite considerable variation between the approaches and the crudeness of some of the simplifying assumptions. This suggests that the overall modelling approach is also relatively robust in its ability to simulate the real system, even though some details may be rather poor approximations to reality. The major features of each approach are summarised in Table 1.

4.2. Comparison of model with existing data

Given that the distance between Fe atoms is around 3.5 Å (0.35 nm) in typical oligomers and solids (Rose

Table 1
Major features of the various approaches to simplifying the relationship between iron precipitation and dissolution kinetics and iron solubility at (pseudo-)equilibrium

Approach	Simplifying assumptions	Solubility relationship when only Fe′ considered dissolved	Solubility relationship when polymers containing $\leqslant p$ Fe atoms considered dissolved
1	Single values of k_f^* and k_d^* for all polymers	$[Fe'] = \frac{k_f^*[Fe]_T}{k_f^*[Fe]_T + k_d^*}$ Hyperbolic; $[Fe'] \approx [Fe]_T$ when $[Fe]_T \ll k_d^*/k_f^*$ and $[Fe'] \approx k_d^*/k_f^*$ when $[Fe]_T \gg k_d^*/k_f^*$	$[Fe_{\leqslant p}]_T = [Fe]_T\left(1 - \left(\frac{[Fe]_T}{[Fe]_T + k_d^*/k_f^*}\right)^p\right)$ $[Fe_{\leqslant p}]_T \approx [Fe]_T$ when $[Fe]_T \ll pk_d^*/k_f^*$ and $[Fe_{\leqslant p}]_T \approx pk_d^*/k_f^*$ when $[Fe]_T \gg pk_d^*/k_f^*$
2	Separate values for homogeneous (k_{f1}^*) and heterogeneous ($k_{f2\to n}^*$) precipitation; single value of k_d^* for all polymers	$[Fe'] = \frac{k_{f2\to n}^*[Fe]_T + k_d^* \pm \sqrt{(k_{f2\to n}^*[Fe]_T - k_d^*)^2 + 4k_{f1}^* k_d^*[Fe]_T}}{2(k_{f2\to n}^* - k_{f1}^*)}$ Quadratic; $[Fe'] \approx [Fe]_T$ when $[Fe]_T \ll k_d^*/k_{f2\to n}^*$ and $[Fe'] \approx k_d^*/k_{f2\to n}^*$ when $[Fe]_T \gg k_d^*/k_{f2\to n}^*$ Approaches exact solubility limit condition as $k_{f1}^* \to 0$	$[Fe_{\leqslant p}]_T = [Fe']\frac{1+\frac{(k_{f1}^* - k_{f2\to n}^*)}{k_d^*}[Fe'] - \frac{k_{f1}^*}{k_{f2\to n}^*}(k_{f2\to n}^*[Fe']/k_d^*)^p}{1-(k_{f2\to n}^*[Fe']/k_d^*)}$ Empirically observed to exhibit "solubility limit" behaviour, but asymptotes are not easily determined As $k_{f1}^* \to 0$, simplifies to an exact (but unrealistic) solubility limit condition where $[Fe_{\leqslant p}]_T = [Fe']$
3	Different values of k_f^* and k_d^* for each polymer, but the same ratio $K^* = k_f^*/k_d^*$ for all polymers	$[Fe'] = \frac{[Fe]_T}{K^*[Fe]_T + 1}$ Hyperbolic; $[Fe'] \approx [Fe]_T$ when $[Fe]_T \ll 1/K^*$ and $[Fe'] \approx 1/K^*$ when $[Fe]_T \gg 1/K^*$	$[Fe_{\leqslant p}]_T = [Fe]_T\left(1 - \left(\frac{[Fe]_T}{[Fe]_T + 1/K^*}\right)^p\right)$ $[Fe_{\leqslant p}]_T \approx [Fe]_T$ when $[Fe]_T \ll p/K^*$ and $[Fe_{\leqslant p}]_T \approx p/K^*$ when $[Fe]_T \gg p/K^*$

et al., 1997a), "truly dissolved" iron (<1 nm in size) could include polymers with up to around 30 atoms (based on a spherical configuration, or less based on planar or linear configurations). Using values of $k_f^* = 4.1 \times 10^7\ M^{-1}\ s^{-1}$ and $k_d^* = 4.8 \times 10^{-6}\ s^{-1}$ for a one week old precipitate in seawater (Rose and Waite, 2003), the calculated equilibrium concentration of Fe′ using Approach 1 is $\log[Fe'] = -12.9$, compared with an equilibrium concentration of "truly dissolved" iron of $\log[Fe_{\leqslant 30}]_T = -11.5$.

On the basis of these calculations, it is possible to reconcile the apparent discrepancy between reported values of iron(III) solubility measured using size fractionation (e.g. from Liu and Millero, 2002) versus values calculated from kinetic parameters (e.g. from Rose and Waite, 2003). The solubility of iron(III) in artificial seawater after the precipitate was aged for one week was calculated by Liu and Millero (2002) using 0.02 μm filtration to be log[dissolved Fe(III)] = −11.0. This value is predicted by our model if polymers of size <90 Fe atoms are considered dissolved. Again assuming that the separation distance between Fe atoms in a typical polymer is around 3.5 Å (Rose et al., 1997a), this would be reasonable if Fe polymers were primarily one dimensional (a one-dimensional polymer with greatest dimension of 1 nm would contain ~60 Fe atoms, a fully two-dimensional circular polymer ~2600 Fe atoms, and a fully three-dimensional spherical polymer ~100,000 Fe atoms). Given that Fe polymers formed at high [OH^-]:[Fe(III)] ratios are generally semi-linear (i.e. branched, but without full two-dimensional character) (Bottero et al., 1991), the value of 90 atoms obtained using our model appears to be in reasonable agreement with mechanistic observations. In addition, it is thought that filter membranes can typically trap particles that are smaller than the nominal membrane pore size due to factors such as electrostatic and hydrophobic interactions between particles and the membrane.

4.3. Ageing of the solid phase (crystal ripening)

Over time, FOP undergoes various physico-chemical changes that decrease the lability of the solid phase (Kuma et al., 1993). This phenomenon of "ageing" results in increasingly crystalline and increasingly thermodynamically stable forms of precipitated iron, such as ferrihydrite, haematite, maghemite, lepidocrocite and goethite (Schwertmann, 1991; Kuma et al., 1993). The fact that such transformations occur indicates that, strictly speaking, equilibrium is not reached for many weeks or perhaps even years; however as noted previously, such transformations typically occur relatively slowly compared to the timescales for precipitation and dissolution and can thus be treated separately to these primary kinetic phenomena.

Kinetically, the most obvious manifestation of FOP ageing is a decrease in the rate constant for FOP dissolution, k_d^*, over time. This phenomenon has been quantified by Kuma and co-workers (Kuma et al., 1992, 1993) and more recently in our work (Rose and Waite, 2003), amongst others. The decrease in k_d^* occurs as a result of two major processes:

1. A decrease in the availability of coordination sites on Fe atoms, as they become increasingly coordinated to other Fe atoms over time via depolymerisation of more labile atoms (whose apparent k_d^* value will be higher due to the requirement for less bond weakening) and subsequent re-polymerisation into more stable coordination environments.
2. Conversion of hydroxy-bridges to oxy-bridges without any change in the coordination environment of Fe atoms.

We have noted that, as water exchange from dissolved $Fe(OH)^0_{3(aq)}$ is the rate-limiting step for polymerisation, the apparent rate constant k_f^* will not be significantly affected by oxolation reactions. However, as with k_d^*, saturation of available coordination sites on Fe atoms over time would be expected to result in a decrease in k_f^*. A comparison of the relationship between iron solubility measured by size-based separation and the dissolution rate of FOP offers some insight into these processes, as shown in Fig. 4. Measured iron solubility as plotted in the figure was determined using a *y*-intercept obtained from iron solubility measurements in NaCl (Liu and Millero, 1999) with a slope obtained from iron solubility measurements in seawater (Liu and Millero, 2002) since there was no published value for the slope in NaCl. Values for k_d^* were taken from Rose and Waite (2003). The decrease in measured iron solubility has a slope that is quite similar to the decrease in k_d^* after the precipitate is 24 h old, but during the initial 24 h after precipitation the value of k_d^* decreases much more rapidly than the overall iron solubility. Thus if the equilibrium solubility of iron is a function of k_d^*/k_f^*, as suggested by our mechanistic approach, the initial rapid decrease in k_d^* during the initial 24 h over and above that after 24 h must be accompanied by a proportional decrease in k_f^* during this time.

Such a scenario corresponds very well to our expectation of the influence of the two factors listed above on each of the parameters k_d^* and k_f^*: the initial decrease, which affects k_d^* and k_f^* proportionately, can be attributed to a decrease in the availability of coordination sites on Fe atoms as they

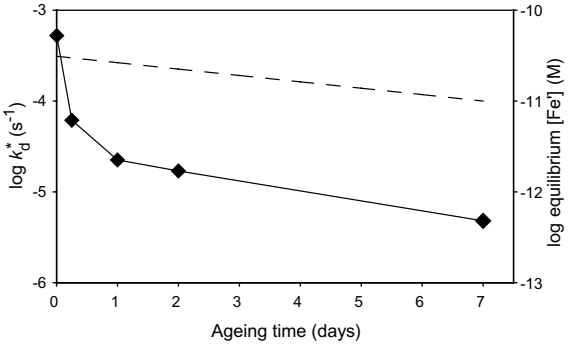

Fig. 4. Change in k_d^*, the rate constant for dissociation of FOP (diamonds and solid line) from the data of Rose and Waite (2003) compared with the equilibrium Fe′ concentration predicted from the data of Liu and Millero (Liu and Millero, 1999, 2002) (dashed line), as a function of FOP age.

become saturated by olation reactions, while the slower decrease, which affects only k_d^*, can be attributed to oxolation by condensation of existing hydroxy-bridges.

Applying this model, we can approximate saturation of coordination sites and oxolation of existing bonds as first-order processes. Since the first process affects the availability of coordination sites for heterogeneous precipitation and for dissolution, at any time we expect only some fraction of the Fe atoms in FOP to be reactive. This process clearly cannot result in all Fe atoms within the FOP becoming unreactive; rather, the fraction of Fe atoms available for reaction approaches some limiting value, denoted by $\alpha_{FOP\infty}$. Consequently, the apparent values of k_f^* and k_d^* approach limiting values of $k_{f\infty}^*$ and $k_{d\infty}^*$, respectively, where $k_{f\infty}^* = k_{f0}^* \alpha_{FOP\infty}$, $k_{d\infty}^* = k_{d0}^* \alpha_{FOP\infty}$, and k_{f0}^* and k_{d0}^* denote the values of k_f^* and k_d^* initially. (In fact $k_{f\infty}^* = k_f^* \alpha_{FeT\infty}$, where $\alpha_{FeT\infty}$ denotes the limiting value for the fraction of total iron that is available for reaction; however we assume here that we are dealing with a saturated system at equilibrium, such that $[Fe'] \ll [Fe]_T$ and hence Fe′ is negligible in this calculation). Denoting the first-order decay constant for the first process as k_1 and for the second process as k_2, we obtain the value of k_f^* as a function of time:

$$\begin{aligned} k_f^*(t) &= k_{f\infty}^* + (k_{f0}^* - k_{f\infty}^*)e^{-k_1 t} \\ &= k_{f0}^* \alpha_{FOP\infty} + (k_{f0}^* - k_{f0}^* \alpha_{FOP\infty})e^{-k_1 t} \\ &= k_{f0}^* \{\alpha_{FOP\infty} + (1 - \alpha_{FOP\infty})e^{-k_1 t}\} \end{aligned} \quad (38)$$

and, similarly, the value of k_d^* as a function of time:

$$\begin{aligned} k_d^*(t) &= \{k_{d\infty}^* + (k_{d0}^* - k_{d\infty}^*)e^{-k_1 t}\}e^{-k_2 t} \\ &= \{k_{d0}^* \alpha_{FOP\infty} + (k_{d0}^* - k_{d0}^* \alpha_{FOP\infty})e^{-k_1 t}\}e^{-k_2 t} \\ &= k_{d0}^* \{\alpha_{FOP\infty} + (1 - \alpha_{FOP\infty})e^{-k_1 t}\}e^{-k_2 t} \end{aligned} \quad (39)$$

Hence the pseudo-equilibrium Fe′ concentration calculated using Approach 1 varies as a function of time according to the relationship:

$$\begin{aligned} [Fe'](t) &= \frac{k_d^*(t)}{k_f^*(t)} = \frac{k_{d0}^* \{\alpha_{APO\infty} + (1 - \alpha_{APO\infty})e^{-k_1 t}\}e^{-k_2 t}}{k_{f0}^* \{\alpha_{FOP\infty} + (1 - \alpha_{FOP\infty})e^{-k_1 t}\}} \\ &= \frac{k_{d0}^*}{k_{f0}^*} e^{-k_2 t} = [Fe']_0 e^{-k_2 t} \end{aligned} \quad (40)$$

where $[Fe']_0$ is the Fe′ concentration at pseudo-equilibrium immediately after precipitation from a homogeneous solution of iron(III). This relationship is consistent with the logarithmic decrease in iron solubility observed by Liu and Millero (2002) shown in Fig. 4. In the form shown in Eq. (40), the equilibrium Fe′ concentration approaches zero at infinite time, which is clearly unrealistic. However it is simple to re-formulate this expression to approach some asymptotic value, which would correspond to the solubility of the most stable form of iron under given conditions, i.e. to the value at true equilibrium. We have not done so here because available data would not allow accurate determination of this value.

Applying this model quantitatively to the data shown in Fig. 4, we obtain a value of $k_2 = 1.9 \times 10^{-6}\ s^{-1}$ from the solubility data of Liu and Millero (Liu and Millero, 1999, 2002) as plotted. From the best fit to the dissolution data, we then obtain values for $k_1 = 1.0 \times 10^{-4}\ s^{-1}$, and

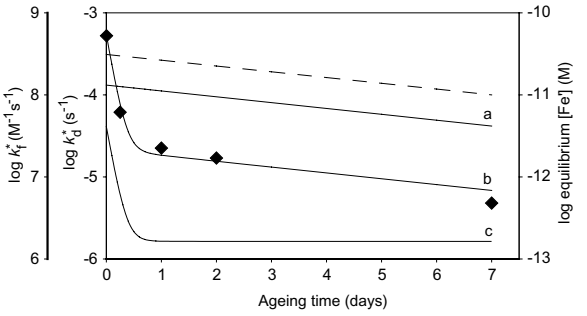

Fig. 5. Model predictions of k_d^*, k_f^* and equilibrium Fe′ concentration as a function of FOP age (solid lines: (a) equilibrium Fe′ concentration; (b) k_d^*; (c) k_f^*). The equilibrium Fe′ concentration predicted from the data of Liu and Millero (Liu and Millero, 1999, 2002) is shown for reference (dashed line), along with the measured values of k_d^* from Rose and Waite (2003) (diamonds).

$\alpha_{FOP\infty} = 0.04$. The fit of the model is shown in Fig. 5. The model fits the measured equilibrium data extremely well, except that it underestimates the iron solubility by around 0.3 log units when using values for $k_{f0}^* = 4.1 \times 10^7\ M^{-1}\ s^{-1}$ and $k_{d0}^* = 5.3 \times 10^{-4}\ s^{-1}$ determined in our previous study (Rose and Waite, 2003). This is expected, given that we are simulating the pseudo-equilibrium [Fe′], rather than the total concentration of Fe atoms in all dissolved polymers. However, it is relatively straightforward to calculate these values from Eq. (34) if desired.

5. CONCLUSIONS

We have described here a polymer-based model for the precipitation of iron(III) oxyhydroxides in aqueous solution, and used this model to reconcile a mechanistic understanding of the processes of precipitation and dissolution from a kinetic perspective with equilibrium measurements of iron(III) solubility. We have also demonstrated the ability of the model to quantitatively explain the effects of precipitate ageing.

Whereas conventional thermodynamic analysis requires separate approaches to dealing with dissolved phase reactions, the existence of pure solid phases in equilibrium with the dissolved phase, and the intermediate behaviour of surface species, the polymer-based approach does not need to differentiate between them. Rather than requiring a special definition of the activity of a solid phase, the activity of surface Fe atoms and pure solid phase Fe atoms is implicitly accounted for by increasing degrees of saturation of coordinative sites. Although the definition of dissolved versus non-dissolved species is not implicitly specified by this approach, it is relatively straightforward to make this distinction in a quantitative manner if a definition is assigned, for example, on the basis of polymer size. The strength of this model lies in its ability to describe equilibrium features of iron(III) hydrolysis and precipitation, and hence maintain consistency with previous thermodynamic analyses, whilst simultaneously providing the mechanistic detail that is necessary to explain the kinetics of iron(III) precipitation and dissolution reactions. The latter feature is essential for

understanding the dynamics of iron biogeochemistry in natural waters, and for the successful predictive modelling of the behaviour of iron in environmental systems.

ACKNOWLEDGMENTS

Comments provided by François Morel on the doctoral dissertation of A.L.R. and comments provided by Mark Benjamin on an earlier draft of this manuscript were of great help in the development of this work. The helpful comments provided by two anonymous reviewers on the initial submission of this manuscript are also gratefully acknowledged.

APPENDIX A. SUPPLEMENTARY DATA

Supplementary data associated with this article can be found, in the online version, at doi:10.1016/j.gca.2007.02.024.

REFERENCES

Blesa M. A. and Matijević E. (1989) Phase transformations of iron oxides, oxohydroxides, and hydrous oxides in aqueous media. *Adv. Colloid Interface Sci.* **29**, 173–221.

Bottero J. Y., Tchoubar D., Arnaud M. and Quienne P. (1991) Partial hydrolysis of ferric nitrate salt. Structural investigation by dynamic light scattering and small-angle X-ray scattering. *Langmuir* **7**, 1365–1369.

Bottero J. Y., Manceau A., Villieras F. and Tchoubar D. (1994) Structure and mechanisms of formation of iron oxide hydroxide (chloride) polymers. *Langmuir* **10**, 316–319.

Byrne R. H. and Kester D. R. (1976) Solubility of hydrous ferric oxide and iron speciation in seawater. *Mar. Chem.* **4**, 255–274.

Byrne R. H., Luo Y.-R. and Young R. W. (2000) Iron hydrolysis and solubility revisited: observations and comments on iron hydrolysis characterizations. *Mar. Chem.* **70**, 23–35.

Combes J. M., Manceau A., Calas G. and Bottero J. Y. (1989) Formation of ferric oxides from aqueous solutions: a polyhedral approach by X-ray absorption spectroscopy: I. Hydrolysis and formation of ferric gels. *Geochim. Cosmochim. Acta* **53**, 583–594.

Cornell R. M. and Schwertmann U. (2004) *The Iron Oxides: Structure, Properties, Reactions, Occurences, Uses*. Wiley-VCH Verlag GmbH & Co..

Crichton R. (2001) *Inorganic Biochemistry of Iron Metabolism: From Molecular Mechanisms to Clinical Consequences*. John Wiley & Sons, Chichester, England.

Doelsch E., Mason A., Rose J., Stone W. E. E., Bottero J. Y. and Bertsch P. M. (2003) Chemistry and structure of colloids obtained by hydrolysis of Fe(III) in the presence of SiO_4 ligands. *Colloids Surf. A: Physicochem. Eng. Aspects* **217**, 121–128.

Dousma J. and De Bruyn P. L. (1976) Hydrolysis-precipitation studies of iron solutions. I. Model for hydrolysis and precipitation from Fe(III) nitrate solutions. *J. Colloid Interface Sci.* **56**, 527–539.

Dousma J., Van den Hoven T. J. and De Bruyn P. L. (1978) The influence of chloride ions on the formation of iron(III) oxyhydroxide. *J. Inorg. Nucl. Chem.* **40**, 1089–1093.

Dousma J., den Ottelander D. and de Bruyn P. L. (1979) The influence of sulfate ions on the formation of iron(III) oxides. *J. Inorg. Nucl. Chem.* **41**, 1565–1568.

Eigen M. and Wilkins R. G. (1965) Kinetics and mechanisms of formation of metal complexes. In *Mechanisms of Inorganic Reactions* (eds. R. K. Marmann, R. T. Fraser, and J. Bouman). American Chemical Society, pp. 55–80.

Fanghänel T. and Neck V. (2002) Aquatic chemistry and solubility phenomena of actinide oxides/hydroxides. *Pure Appl. Chem.* **74**, 1895–1907.

Flory P. J. (1946) Fundamental principles of condensation polymerization. *Chem. Rev.* **39**, 137–197.

Flynn, Jr., C. M. (1984) Hydrolysis of inorganic iron(III) salts. *Chem. Rev.* **84**, 31–41.

Grundl T. and Delwiche J. (1993) Kinetics of ferric oxyhydroxide precipitation. *J. Contam. Hydrol.* **14**, 71–87.

Jolivet J.-P., Tronc E. and Chaneac C. (2006) Iron oxides: from molecular clusters to solid. A nice example of chemical versatility. *C. R. Geosci.* **338**, 488–497.

Kuchanov S., Slot H. and Stroeks A. (2004) Development of a quantitative theory of polycondensation. *Prog. Polym. Sci.* **29**, 563–633.

Kuma K., Suzuki Y. and Matsunaga K. (1993) Solubility and dissolution rate of colloidal γ-FeOOH in seawater. *Water Res.* **27**, 651–657.

Kuma K., Nishioka J. and Matsunaga K. (1996) Controls on iron(III) hydroxide solubility in seawater: the influence of pH and natural organic chelators. *Limnol. Oceanogr.* **41**, 396–407.

Kuma K., Nakabayashi S., Suzuki Y. and Matsunaga K. (1992) Dissolution rate and solubility of colloidal hydrous ferric oxide in seawater. *Mar. Chem.* **38**, 133–143.

Kuma K., Katsumoto A., Kawakami H., Takatori F. and Matsunaga K. (1998) Spatial variability of Fe(III) hydroxide solubility in the water column of the northern North Pacific Ocean. *Deep-Sea Res. Part I Oceanogr. Res. Pap.* **45**, 91–113.

Liu X. and Millero F. J. (1999) The solubility of iron hydroxide in sodium chloride solutions. *Geochim. Cosmochim. Acta* **63**, 3487–3497.

Liu X. and Millero F. J. (2002) The solubility of iron in seawater. *Mar. Chem.* **77**, 43–54.

Meakin P. (1984) Effects of cluster trajectories on cluster–cluster aggregation: a comparison of linear and Brownian trajectories in two- and three-dimensional simulations. *Phys. Rev. A* **29**, 997.

Millero F. J. (1998) Solubility of Fe(III) in seawater. *Earth Planet. Sci. Lett.* **154**, 323–329.

Millero F. J., Wensheng Y. and Aicher J. (1995) The speciation of Fe(II) and Fe(III) in natural waters. *Mar. Chem.* **50**, 21–39.

Perera W. N. and Hefter G. (2003) Mononuclear cyano- and hydroxo-complexes of iron(III). *Inorg. Chem.* **42**, 5917–5923.

Pham A. N., Rose A. L., Feitz A. J. and Waite T. D. (2006) Kinetics of Fe(III) precipitation in aqueous solutions at pH 6.0–9.5 and 25 °C. *Geochim. Cosmochim. Acta* **70**, 640–650.

Rose A. L. and Waite T. D. (2003) Kinetics of hydrolysis and precipitation of ferric iron in seawater. *Environ. Sci. Technol.* **37**, 3897–3903.

Rose J., Manceau A., Bottero J. Y., Masion A. and Garcia F. (1996) Nucleation and growth mechanisms of Fe oxyhydroxide in the presence of PO_4 ions. 1. Fe K-Edge EXAFS study. *Langmuir* **12**, 6701–6707.

Rose J., Manceau A., Masion A. and Bottero J. Y. (1997a) Structure and mechanisms of formation of $FeOOH(NO_3)$ oligomers in the early stages of hydrolysis. *Langmuir* **13**, 3240–3246.

Rose J., Flank A. M., Masion A., Bottero J. Y. and Elmerich P. (1997b) Nucleation and growth mechanisms of Fe oxyhydroxide in the presence of PO_4 ions. 2. P K-Edge EXAFS study. *Langmuir* **13**, 1827–1834.

Schwertmann U. (1991) Solubility and dissolution of iron oxides. In *Iron Nutrition and Interactions in Plants* (eds. Y. Chen and Y. Hadar). Kluwer Academic Publishers, The Netherlands, pp. 3–27.

Schwertmann U., Friedl J. and Stanjek H. (1999) From Fe(III) ions to ferrihydrite and then to hematite. *J. Colloid Interface Sci.* **209**, 215–223.

Sommer B. A. and Margerum D. W. (1970) Kinetic study of the hydroxoiron(III) dimer. *Inorg. Chem.* **9**, 2517–2521.

Stumm W. (1992) *Chemisty of the Solid–Water Interface: Processes at the Mineral–Water and Particle–Water Interface in Natural Systems*. John Wiley & Sons.

Stumm W. (1997) Reactivity at the mineral–water interface: dissolution and inhibition. *Colloids Surf. A: Physicochem. Eng. Aspects* **120**, 143–166.

Sunda W. G. and Huntsman S. A. (1998) Processes regulating cellular metal accumulation and physiological effects: phytoplankton as model systems. *Sci. Total Environ.* **219**, 165–181.

Sunda W. G. and Huntsman S. A. (2003) Effect of pH, light, and temperature on Fe-EDTA chelation and Fe hydrolysis speciation in seawater. *Mar. Chem.* **84**, 35–47.

Tchoubar D., Bottero J. Y., Quienne P. and Arnaud M. (1991) Partial hydrolysis of ferric chloride salt. Structural investigation by photon-correlation spectroscopy and small-angle x-ray scattering. *Langmuir* **7**, 398–402.

Zinder B., Furrer G. and Stumm W. (1986) The coordination chemistry of weathering: II. Dissolution of Fe(III) oxides. *Geochim. Cosmochim. Acta* **50**, 1861–1869.

Associate editor: Robert H. Byrne